

This discussion paper is/has been under review for the journal Atmospheric Measurement Techniques (AMT). Please refer to the corresponding final paper in AMT if available.

**Towards IASI-New Generation (IASI-NG):
impact of improved
spectral resolution**

C. Crevoisier et al.

Towards IASI-New Generation (IASI-NG): impact of improved spectral resolution and radiometric noise on the retrieval of thermodynamic, chemistry and climate variables

C. Crevoisier¹, C. Clerbaux², V. Guidard³, T. Phulpin⁴, R. Armante¹, B. Barret⁵,
C. Camy-Peyret⁶, J.-P. Chaboureau⁵, P.-F. Coheur⁷, L. Crépeau¹, G. Dufour⁸,
L. Labonnote⁹, L. Lavanant¹⁰, J. Hadji-Lazaro², H. Herbin⁹,
N. Jacquinet-Husson¹, S. Payan², E. Péquignot⁴, C. Pierangelo⁴, P. Sellitto^{8,*},
and C. Stubenrauch¹

¹Laboratoire de Météorologie Dynamique, IPSL, CNRS – UMR8539, Ecole Polytechnique, Palaiseau, France

²UPMC Université Paris 6, Université Versailles St-Quentin, CNRS-INSU, LATMOS-IPSL, Paris, France

³Météo-France and CNRS/CNRM-GAME, Toulouse, France

⁴Centre National d'Etudes Spatiales (CNES), Toulouse, France

⁵Laboratoire d'Aérodynamique/OMP, Université de Toulouse, Toulouse, France

Title Page

Abstract

Introduction

Conclusions

References

Tables

Figures

⏪

⏩

◀

▶

Back

Close

Full Screen / Esc

Printer-friendly Version

Interactive Discussion



Abstract

Besides their strong contribution to weather forecast improvement through data assimilation, thermal infrared sounders onboard polar-orbiting platforms are now playing a key role for monitoring atmospheric composition changes. The Infrared Atmospheric Sounding Interferometer (IASI) instrument developed by the French space agency (CNES) and launched by Eumetsat onboard the Metop satellite series is providing essential inputs for weather forecasting and pollution/climate monitoring owing to its smart combination of large horizontal swath, good spectral resolution and high radiometric performance. EUMETSAT is currently preparing the next polar-orbiting program (EPS-SG) with the Metop-SG satellite series that should be launched around 2020. In this framework, CNES is studying the concept of a new instrument, the IASI-New Generation (IASI-NG), characterized by an improvement of both spectral and radiometric characteristics as compared to IASI, with three objectives: (i) continuity of the IASI/Metop series; (ii) improvement of vertical resolution; (iii) improvement of the accuracy and detection threshold for atmospheric and surface components. In this paper, we show that an improvement of spectral resolution and radiometric noise fulfill these objectives by leading to (i) a better vertical coverage in the lower part of the troposphere, thanks to the increase in spectral resolution; (ii) an increase in the accuracy of the retrieval of several thermodynamic, climate and chemistry variables, thanks to the improved signal-to-noise ratio as well as less interferences between the signatures of the absorbing species in the measured radiances. The detection limit of several atmospheric species is also improved. We conclude that IASI-NG has the potential for strongly benefiting the numerical weather prediction, chemistry and climate communities now connected through the European GMES/Copernicus initiative.

Towards IASI-New Generation (IASI-NG): impact of improved spectral resolution

C. Crevoisier et al.

Title Page

Abstract

Introduction

Conclusions

References

Tables

Figures

⏪

⏩

◀

▶

Back

Close

Full Screen / Esc

Printer-friendly Version

Interactive Discussion



1 Introduction

Infrared sounders are a key element of space observation of the Earth system. They enable the monitoring of several thermodynamic, chemistry and climate variables over land and sea, night and day. In particular, the Infrared Atmospheric Sounding Interferometer (IASI) (Chalon et al., 2011), flying onboard Metop-A since October 2006 and Metop-B since September 2012, has demonstrated the possibility to retrieve or detect several chemistry and climate variables from hyperspectral infrared observation: for instance water vapour (H₂O), carbon dioxide (CO₂), carbon monoxide (CO), methane (CH₄), ozone (O₃), sulfur dioxide (SO₂), hydrogen sulfide (H₂S), ammonia (NH₃), nitric acid (HNO₃), volatile organic compounds (VOCs), aerosols, etc. (Hilton et al., 2012; Clarisse et al., 2011) on regional and global scales. IASI has given access to species that had never previously been observed from space on a global scale (Clarisse et al., 2009; Razavi et al., 2011; Dufлот et al., 2013) and enables the monitoring of key gases for climate and atmospheric chemistry in quasi near real time. IASI has also highlighted the benefit of high-performance infrared sounders for numerical weather prevision (NWP) applications: IASI on Metop-A currently contributes more impact than any instrument on any satellite to the skill of the 24h global forecast of several NWP centers (Météo-France, UK MetOffice, ECMWF) (Collard and McNally, 2009; Guidard et al., 2011, J. Eyre, personal communication, 2011).

Despite their good spatial and temporal coverage and their essential contribution to the three dimensional characterization of the atmosphere, infrared sounders still suffer from a limited sensitivity to the lower part of the troposphere near the surface. For instance, with existing instruments, it is still challenging to identify temperature inversions or to retrieve with an adequate precision water vapour near the surface where it is the most abundant. Similarly, the measurement of the atmospheric concentration of short-lived species that are rapidly deposited or destroyed by chemical reactions in the atmosphere (e.g. NH₃, methanol, etc.) remains difficult since (i) their concentrations are highest near the surface; (ii) their low abundance is such that their spectral

AMTD

6, 11215–11277, 2013

Towards IASI-New Generation (IASI-NG): impact of improved spectral resolution

C. Crevoisier et al.

Title Page

Abstract

Introduction

Conclusions

References

Tables

Figures



Back

Close

Full Screen / Esc

Printer-friendly Version

Interactive Discussion

IRS2b and IRS2c will assume a spectral resolution of 0.25 cm^{-1} (Gaussian apodization) and the same three noise scenarios. As can be seen from Fig. 1, the IASI-NG objective and threshold radiometric noises (recommended upper and lower limit for noise specifications) pretty much cover the range of these scenarios.

2.2 Channel sensitivities to atmospheric and surface variables

Before performing the retrievals of atmospheric variables, the first step in evaluating the capability of an infrared sounder to retrieve these variables consists in identifying the spectral regions offering the optimal characteristics for the retrieval. Three criteria might be used: the target signal must be the highest possible, the target signal must be greater than the signals due to other variables (these will be called ‘interferences’ in the following), and the channels must harmoniously cover the whole atmospheric column. To evaluate the impact of improved spectral resolution and radiometric noise on the two first criteria, we focus here on the sensitivity of the channels to major atmospheric and surface variables.

For a given atmospheric situation, the variation of the brightness temperature induced by a given variation of atmospheric and surface variables have been computed as

$$\Delta \text{BT}(v, \Delta T) = \sum_{j=1}^{nl} \frac{\partial \text{BT}}{\partial T}(v, j) \times \Delta T(j) \text{ for temperature} \quad (2)$$

$$\Delta \text{BT}(v, \Delta q_{\text{gas}}) = \sum_{j=1}^{nl} \frac{\partial \text{BT}}{\partial q_{\text{gas}}}(v, j) \times \Delta q_{\text{gas}}(j) \text{ for a gas} \quad (3)$$

where $\frac{\partial \text{BT}}{\partial T}(v, j)$ and $\frac{\partial \text{BT}}{\partial q_{\text{gas}}}(v, j)$ are respectively the temperature and gas Jacobians at pressure level j and nl is the number of pressure layers.

Figure 2 displays the channel sensitivity for the spectral resolution of IASI (IRS1a, b, c scenarios) and IASI-NG (IRS2a, b, c scenarios) to typical variations of the major

Towards IASI-New Generation (IASI-NG): impact of improved spectral resolution

C. Crevoisier et al.

Title Page

Abstract

Introduction

Conclusions

References

Tables

Figures

⏪

⏩

◀

▶

Back

Close

Full Screen / Esc

Printer-friendly Version

Interactive Discussion



Towards IASI-New Generation (IASI-NG): impact of improved spectral resolution

C. Crevoisier et al.

Title Page

Abstract

Introduction

Conclusions

References

Tables

Figures

⏪

⏩

◀

▶

Back

Close

Full Screen / Esc

Printer-friendly Version

Interactive Discussion

remains quite challenging. However, the resulting errors depend on the chosen a priori. Therefore, it is not their absolute values that should be considered but their values from one scenario relative to another. It must also be kept in mind that the error reduction brought by a given instrument is overestimated since these values are based on the use of all channels and errors from radiative transfer modeling, cloud residuals, or calibration are not taken into account.

First, only the band $645\text{--}770\text{ cm}^{-1}$ is used in the retrieval procedure. As said in Sec. 3.1.1, the Jacobians of the corresponding channels do not peak at the surface. Therefore no information on the surface will be brought by this band alone. The number of degrees of freedom for each scenario is given in Table 2. The greater the spectral resolution and the lower the noise, the higher the number of DOFs. The number of DOFs for IASI (IRS1a) is low, highlighting the good a priori knowledge on temperature stemming from the assimilation of several observations. The better performance of the IRS2 scenarios as compared to IASI does not come only from the improved noise (IRS1b is worse than IRS2b), but neither from the greater resolution alone (IRS2b is similar to IRS1c). Taking into account the sole radiometric noise or also adding the uncertainties in water vapour and surface characteristics does not change this result.

The relative gain in retrieval uncertainty to the a priori is given by the difference between the a posteriori and the a priori errors, normalized by the a priori error. It is plotted in Fig. 5a. A factor of $\sim 1.5/2$ depending on the altitude is well seen between IRS1a-IASI (dashed blue line) and the IRS2a (full blue line) scenario. At 500 hPa, the gain is 20% for IRS2a compared to 12% for IRS1a-IASI. The comparison between IRS2a and IRS1b or IRS1c reveals that a greater spectral resolution brings a significant improvement in addition to the one stemming from the reduction of the radiometric noise.

Second, a combination of the two bands $645\text{--}770\text{ cm}^{-1}$ and $2250\text{--}2420\text{ cm}^{-1}$ is used. Both the number of DOFs and the relative gain are close even if better than when using the first band alone. The difference comes from the lower part of the troposphere as seen in Fig. 5b. Near the surface, the improvement is significantly better,

as expected from the better coverage of this part of the atmospheric column by the temperature Jacobians (Fig. 4). Moreover, the reduction of the noise by a factor better than 2 (IRS1c and IRS2c) compared to IRS1a-IASI strongly improves the retrieval near the surface, highlighting that the reduction of the noise in that part of the spectrum is particularly relevant.

3.2 Water vapour

3.2.1 Sensitivity of IASI and IASI-NG channels to water vapour

As seen in Fig. 2, H₂O absorption lines span the entire spectral range covered by IASI, with the ν_2 absorption band extending from 1200 to 2150 cm⁻¹. Between 800 and 1200 cm⁻¹, the water vapour continuum is particularly important. The spectral range between 1400 and 2150 cm⁻¹ is the most sensitive to water vapour variation (with a signal around 1.5 K for a variation of 20% in Fig. 2). In the regions below 770 cm⁻¹ and between 950 and 1050 cm⁻¹ CO₂ and O₃ interfering absorption lines are found and the channel sensitivity to a 20% variation of H₂O is lower than 0.5 K. Moreover, these lines are saturated and could potentially induce a bias or large uncertainties on retrieved quantities. Therefore, to retrieve atmospheric water vapour information from high resolution thermal infrared measurements, many previous studies using various instruments such as IMG (Zakharov et al., 2004; Herbin et al., 2007), TES (Worden et al., 2006), or IASI (Herbin et al., 2009; Lacour et al., 2012) have restricted the retrieval spectral range to between 1100 and 1400 cm⁻¹.

Figure 6 represents the half-height widths and altitudes of the maximum of the H₂O Jacobians for the water vapour full absorption band. Within this spectral range, the Jacobians reach all pressure levels from 800 to 100 hPa (2 to 16 km). However, the maxima of water vapour Jacobians cover a wider range of pressure levels for the IRS2-IASI-NG scenarios thanks to their higher spectral resolution. They are also better distributed along the vertical. The number of channels with large Jacobian values at high altitudes is larger, particularly in the 1500–2150 cm⁻¹ spectral band.

Towards IASI-New Generation (IASI-NG): impact of improved spectral resolution

C. Crevoisier et al.

Title Page

Abstract

Introduction

Conclusions

References

Tables

Figures

◀

▶

◀

▶

Back

Close

Full Screen / Esc

Printer-friendly Version

Interactive Discussion



mission with a similar approach, will help minimizing the risk of strong inter-instrument bias, thus complying to the GCOS principles. Assuming that IASI-NG will present the same outstanding spectral and radiometric stability than IASI, it will also strongly contribute the GSICS (Global Space-based Inter-Calibration System, <http://gsics.wmo.int>) effort.

In the following sections, we will focus on three ECVs: CO₂, CH₄ and surface characteristics. Despite the fact that infrared remote sensing provides a way to characterize clouds and aerosols, as well as the thermal part of their total radiative forcing, the study of the impact of improved spectral and radiometric characteristics on their retrieval requires extensive study of several types of particles in non-clear situations (ie taking diffusion into account), inducing heavy computation. This will thus be addressed in a following paper.

4.1 Carbon dioxide

4.1.1 Sensitivity of IASI and IASI-NG channels to CO₂

CO₂ has three absorption bands in the part of the spectrum covered by the instruments: the ν_2 band centered at 667.4 cm⁻¹ (15 μ m), the ν_3 band centered at 2349.2 cm⁻¹ (4.3 μ m), and the weakest laser band centered at 1064 cm⁻¹ (9.4 μ m). In the latter region, the channel sensitivity to CO₂ variations is very low and the interferences with other species (H₂O, O₃) are quite high, preventing the use of the corresponding channels in the retrieval of CO₂. In the two other regions, the CO₂ signature for a 1 % variation comes to 0.15 K at 15 μ m and 0.2 K at 4.3 μ m. In comparison, a 1 K variation of the atmospheric temperature yields a variation of BT between 0.7 and 0.9 K at 15 μ m and 0.7 and 1 K at 4.3 μ m. Any CO₂ retrieval thus requires the decorrelation between temperature and CO₂ signals. In order to make this possible, channels with the lowest sensitivity to other components must be found (Chédin et al., 2003; Crevoisier et al., 2003).

Towards IASI-New Generation (IASI-NG): impact of improved spectral resolution

C. Crevoisier et al.

Title Page

Abstract

Introduction

Conclusions

References

Tables

Figures

⏪

⏩

◀

▶

Back

Close

Full Screen / Esc

Printer-friendly Version

Interactive Discussion



Towards IASI-New Generation (IASI-NG): impact of improved spectral resolution

C. Crevoisier et al.

Title Page

Abstract

Introduction

Conclusions

References

Tables

Figures

◀

▶

◀

▶

Back

Close

Full Screen / Esc

Printer-friendly Version

Interactive Discussion



In these regions, temperature signal is about 0.8 to 0.9 K, and the radiometric noise, which is much lower than the CH₄ signal, should not greatly impact the retrieval. The CH₄ Jacobians for these channels peak at 250 hPa and cover the range 150–500 hPa.

In the ν_3 absorption band at 3.3 μm , which gives access to channels sensitive to the lower troposphere, atmospheric and surface temperatures, emissivity and reflectivity have the major impact and dominate the CH₄ signal. Hence, the use of this band, which is also sensitive to solar radiation, requires a good knowledge of surface characteristics. Moreover, the CH₄ signal is much lower than the radiometric noise whatever the scenario is, except beyond 2700 cm^{-1} where it is lower by a factor of 2 to (of the same level as) the noise improved by a factor of 2 (Eq. 4). Retrieving CH₄ atmospheric content from this part of the spectrum, which is also strongly sensitive to solar radiation, will thus remain very challenging and will only be possible in particular conditions. In the following, results are presented for the 7.7 μm band only.

4.2.2 Impact of spectral resolution and radiometric noise on the retrieval of CH₄

Using the non linear inference scheme described in Sect. 2.3.2 and described in detail in Crevoisier et al. (2009b), we now study the impact of improving the spectral resolution and the radiometric noise on the retrieval of a CH₄ mid-tropospheric integrated content. The results are given in Table 5. Contrary to CO₂, reducing the radiometric noise does not impact much the retrieval error. This is because the IASI radiometric noise is already much lower than the CH₄ signal. On the other hand, by giving access to more channels with reduced sensitivity to water vapour, decreasing the spectral resolution improves the retrieval by decreasing the error by $\sim 40\%$. The CH₄ weighting functions (not shown) are very similar whatever the scenario is with a maximum sensitivity near 250 hPa, with a covering range between 100–500 hPa.

4.3 Surface spectral emissivity

The MultiSpectral Method (MSM) currently used for retrieving mean surface skin temperature and emissivity spectra from 3.7 to 14 μm at a resolution of 0.05 μm from IASI (Pequignot et al., 2008; Capelle et al., 2012) was used to evaluate the expected performance of each scenario on the retrieval of spectral emissivity. As described in these papers, the standard deviation of the method is evaluated using a large set of synthetic simulations comprised of a randomly selected atmospheric situation from the TIGR database, an emissivity spectrum from a laboratory emissivity database and a surface temperature randomly selected within a realistic range.

Figure 10 displays the mean of the difference between the retrieved emissivity spectra and the reference ones averaged over the set of simulations for the IRS1a, b and c scenarios. For IRS1a-IASI, the standard deviation estimated for the spectral emissivity varies from about 0.01–0.015 % for the 10.5–14 and 5.5–8 μm windows to about 0.04–0.05 around 4 μm . The error is at its maximum in the two Reststrahlen bands, around 8–10 and 4 μm , because of (i) the higher emissivity variability; (ii) the higher impact of errors in the thermodynamic characterization of the atmosphere; (iii) a higher radiometric noise (see Fig. 1). Therefore, reducing the noise helps decreasing the error: as seen in Fig. 10, a reduction of the radiometric noise by a factor of 2 (Eq. 4) decreases the error by 1.4 (1.6) at 12 μm and by 1.3 (1.7) at 4 μm . However, increasing the spectral resolution does not change the results since the channels used in the MSM method show similar characteristics for IRS1 or IRS2 scenarios.

5 Atmospheric chemistry

In this section, thermal infrared spectra are analyzed for monitoring tropospheric composition and for the study of its rapid changes. Carbon monoxide, ozone, ammonia and sulfur dioxide are among the key products observed by the IASI mission (Clerbaux et al., 2009; Clarisse et al., 2009). Global and local distributions of trace gases

Towards IASI-New Generation (IASI-NG): impact of improved spectral resolution

C. Crevoisier et al.

Title Page

Abstract

Introduction

Conclusions

References

Tables

Figures

⏪

⏩

◀

▶

Back

Close

Full Screen / Esc

Printer-friendly Version

Interactive Discussion



are routinely derived using several inverse radiative transfer codes depending on the application (global maps, local profiles, or detection of special events).

As described in the previous sections the different noise/spectral resolution scenarios for IASI-NG (see Table 1) are used to simulate IASI-NG like spectra in order to assess the potential improvement for trace gas retrieval or detection. For air pollution studies, improvement in terms of accuracy and also the ability to sound lower in the atmosphere are of particular interest. In the following, the retrieval procedure is based on the optimal estimation method described in Sect. 2.3.1 with error covariance matrices from Hurtmans et al. (2012): results for O_3 and CO are provided with DOFs as a metric to quantify the improvement in terms of vertical information, and retrieval errors are estimated for different layers of the atmosphere and reported relative to IRS1a-IASI.

5.1 Carbon monoxide

5.1.1 Sensitivity of IASI and IASI-NG channels to CO

The absorption band of carbon monoxide (CO) covers the range 2080 to 2200 cm^{-1} . CO absorbs the infrared radiation mainly in its 1-0 vibrational band, centred near 2140 cm^{-1} (Fig. 11). The spectral region has interferences with lines associated with H_2O , CO_2 , N_2O , and O_3 absorption (Fig. 2). At the IASI IRS1 spectral resolution, all channels suffer from weak to medium contamination from these absorbing molecules. The CO content is retrieved using the 2143–2181.25 cm^{-1} spectral range, which offers the best compromise between information content and interferences with other gases (De Wachter et al., 2012). As can be seen from Fig. 11, by increasing the spectral resolution, the lines are better resolved, yielding an increased information content for CO. This is in agreement with results comparing the capability of AIRS and IASI instruments to retrieve CO (George et al., 2009; Thonat et al., 2012).

Towards IASI-New Generation (IASI-NG): impact of improved spectral resolution

C. Crevoisier et al.

Title Page

Abstract

Introduction

Conclusions

References

Tables

Figures

◀

▶

◀

▶

Back

Close

Full Screen / Esc

Printer-friendly Version

Interactive Discussion

Towards IASI-New Generation (IASI-NG): impact of improved spectral resolution

C. Crevoisier et al.

Title Page

Abstract

Introduction

Conclusions

References

Tables

Figures

⏪

⏩

◀

▶

Back

Close

Full Screen / Esc

Printer-friendly Version

Interactive Discussion



between IASI and MOZAIC profiles was much better during late spring summer when CO concentrations are lower and the thermal contrast is higher. We have therefore selected two MOZAIC Frankfurt profiles representative of these contrasted conditions in order to highlight the differences between the 6 scenarios. As seen in Fig. 12, there is a significant impact near the surface, in particular for the little favourable polluted winter case (left): a value of 270 ppbv is retrieved at 1 km, which is close to the MOZAIC measured value of 265 ppbv, whereas the CO retrieved with the IRS1a scenario is too low, at 177 ppbv only (close to the a priori value of 130 ppbv), as observed with IASI. This is in agreement with a higher DOFs for IRS2b (2.4 for this case) than for IRS1a (1.9 for this case). However, due to the still limited vertical resolution, a positive bias is seen at 2-3 km for the IRS2b scenario. Even for the more favourable case of 26 May (Fig. 12, right panel), the IRS2b scenario gives much better results than the IRS1a scenario at all altitudes with DOFs reaching 3 and 2.3, respectively.

5.2 Ozone

5.2.1 Sensitivity of IASI and IASI-NG channels to ozone

In the thermal infrared, ozone (O_3) has two absorption bands, the strongest one near 1042 cm^{-1} (ν_3 $9.7\text{ }\mu\text{m}$ band) and a weaker one centered at 701 cm^{-1} (ν_2) where ozone signatures are mixed with those of H_2O and CO_2 (Fig. 2). The most prominent band extends from 980 to 1100 cm^{-1} (see Fig. 13). It is only slightly perturbed by other weak absorption features of H_2O and CO_2 . Previous experience has demonstrated that the TIR measurements provide information on the ozone vertical profile from the ground up to an altitude of about 40 km, with a maximum sensitivity located in the mid-troposphere (Worden et al., 2007; Boynard et al., 2009; Dufour et al., 2012). The density of the spectra makes it difficult to discriminate individual lines and hence information in the boundary layer can hardly be obtained.

5.2.2 Retrieval of ozone

Improvement in terms of errors and vertical information for the different scenarios and atmospheric scenarios are summarized in Tables 8 and 9. It is well seen that improving spectral resolution and radiometric noise improves the vertical sensitivity, and that most of the improvement in terms of accuracy is in the 0–6 km layer. In the lower atmosphere, between the surface and 2 km, there is only a limited improvement when the instrumental specifications are improved, except when both the signal/noise and spectral resolution are optimized (IRS2c). This is due to the fact that the ozone radiance channels are sensitive to several atmospheric layers and the density of the lines makes it hard to discriminate contributions from near the ground and above. On average, the DOFs for IRS1a-IASI is around 4 pieces of independent information. It increases to 5 for the best case scenario (IRS2c).

For air quality purposes, there is a need to discriminate tropospheric ozone from stratospheric ozone, which is a complicated task using nadir thermal infrared sounder as there is a major absorption contribution due to high levels of stratospheric ozone encountered along the optical path. For most of the atmospheric situations, with a noticeable exception for high thermal contrast cases, tropospheric columns are associated with DOFs lower than one, which means that part of the information in the retrieved tropospheric product comes from the a priori information. In order to investigate how increasing the spectral resolution and reducing the radiometric noise helps to improve this situation, a variant of OEM, based on an altitude-dependent Tikhonov-Philips regularization matrix (Kulawik et al., 2006; Eremenko et al., 2008) instead of an a priori covariance matrix, has also been used (Sellitto et al., 2013). Simulations were done to evaluate the tropospheric ozone distributions as observed over Europe using a regional model, both for the IRS1a/IASI case and the improvement by a factor of 2 for spectral resolution and signal to noise ratio (IRS2b scenario). Figure 14 provides the DOFs (top panels) associated with the (0–6) km columns for a polluted case over Europe, as well as the maximum altitude (bottom panels) for the corresponding averaging kernel. It can

AMTD

6, 11215–11277, 2013

Towards IASI-New Generation (IASI-NG): impact of improved spectral resolution

C. Crevoisier et al.

Title Page

Abstract

Introduction

Conclusions

References

Tables

Figures

◀

▶

◀

▶

Back

Close

Full Screen / Esc

Printer-friendly Version

Interactive Discussion



be seen that the 0–6 km DOFs exceeds one for the IRS2b simulation, with associated maximum sensitivities lower in the atmosphere (2 to 4 km instead of 5 km or higher).

5.3 Detection limits for weak absorbers

Recent studies have shown that by exploiting weak absorption lines observed in the IASI spectra, total columns can also be retrieved for less abundant gases such as sulfur dioxide, ammonia, methanol, formic acid, etc. (Clarisse et al., 2011). It is especially the case when special events happen, such as volcanic eruption, large fires and pollution events, for which a series of molecules can be retrieved simultaneously (e.g. Coheur et al., 2009; R'Honi et al., 2013). The associated errors are rather large as the signal barely exceeds the noise level.

In the following, simulations were performed in order to determine the potential improvement in terms of detection limits when increasing the radiometric and spectral resolution performance. Different atmospheric situations were investigated. The figures provided here are for the tropical case situation, for which the impact of water vapour lines interferences is the strongest.

5.3.1 Sulfur dioxide (SO₂)

SO₂ absorbs thermal infrared radiation in the ν_1 band around 1150 cm^{-1} , the ν_3 band around 1350 cm^{-1} , and the $\nu_1 + \nu_3$ band around 2500 cm^{-1} (Clarisse et al., 2012). The ν_3 band is the most prominent but lies in a range where strong absorptions by methane and water vapour occur, which makes it difficult to accurately retrieve tropospheric SO₂ concentrations.

Figure 15 illustrates the gain in the detection, as a function of altitude, obtained when using the ν_1 , the ν_3 , and the $\nu_1 + \nu_3$ bands. The simulations were performed as follows: different brightness temperature spectra were generated by increasing the SO₂ volume mixing ratio at different altitudes, in order to access the sensitivity at each altitude for different concentrations. The impact is checked using different channels, which

Towards IASI-New Generation (IASI-NG): impact of improved spectral resolution

C. Crevoisier et al.

Title Page

Abstract

Introduction

Conclusions

References

Tables

Figures

⏪

⏩

◀

▶

Back

Close

Full Screen / Esc

Printer-friendly Version

Interactive Discussion



Towards IASI-New Generation (IASI-NG): impact of improved spectral resolution

C. Crevoisier et al.

Title Page

Abstract

Introduction

Conclusions

References

Tables

Figures

⏪

⏩

◀

▶

Back

Close

Full Screen / Esc

Printer-friendly Version

Interactive Discussion

absorption lines of various gases located in the same spectral range interfere with each other (e.g. H₂O for the retrieval of CO and CH₄). Reducing the interferences thus leads to better accuracy. A higher spectral resolution also induces a better vertical resolution thanks to thinner weighting functions and Jacobians (e.g. temperature, CO). On the other hand, reducing the noise particularly matters for variables for which typical variations of brightness temperatures are of the level or much lower than the radiometric noise (CO₂, emissivity, and weak absorbers such as SO₂ and NH₃). Improving the radiometric noise thus yields improved signal/noise ratio, and translates into more accuracy for the retrieved variables, and more sensitivity lower in the atmosphere (e.g. T, H₂O, O₃). It should also lead to the detection of new “unexpected” species currently hidden in the noise, especially in large pollution plumes. Finally, at the moment the shortwave part of the spectrum covered by IASI is not well exploited because of noise issues. This study demonstrates that the noise reduction envisaged for IASI-NG is important as channels in this spectral range present sensitivity to the lower part of the troposphere. Being also able to use them in retrieval or assimilation procedures will thus further improve vertical resolution and accuracy in that part of the atmosphere.

This study has focused on the retrieval of each variable in a stand-alone approach, without taking into account the improvement brought simultaneously on every variable. This will require performing Observing System Simulation Experiments (OSSEs) (e.g. Edwards et al., 2009). In particular, the expected improvement on the characterization of thermodynamic profiles and surface properties (spectral emissivity and surface temperature) will positively impact the retrievals of other atmospheric variables (e.g. trace gases) which usually require a good knowledge of the thermodynamic state of the atmosphere and the surface. It will also benefit several applications based on the retrieved level 2 products. For instance, the detection of ice supersaturation (relative humidity with respect to ice (RH_{ice}) exceeding 100 %), which is a necessary condition for ice nucleation as well as for the persistence of condensation trails induced by air traffic (Lamquin et al., 2012), will be improved thanks to the expected improvement of

the retrieval of water vapour, as shown by a preliminary comparison between AIRS and IASI (Stubenrauch et al., 2012).

With the planned launch of three successive instruments onboard the Metop-SG satellite suites, the IASI-NG mission will extend the IASI series and, thanks to enhancements in both spectral resolution and radiometric noise, will give access to better resolved and more accurate atmospheric and surface variable. IASI-NG will thus strongly benefit the numerical weather prediction, chemistry and climate communities now connected through the European GMES/Copernicus initiative.

Acknowledgements. This research has received funding from CNES. The authors particularly wish to thank the IASI-NG Project Team at CNES and the EPS-SG team at EUMETSAT for fruitful discussions. Calculations were performed at IDRIS, the computer centre of CNRS, and at ClimServ, the data and computer centre of IPSL.



The publication of this article is financed by CNRS-INSU.

References

- Boynard, A., Clerbaux, C., Coheur, P.-F., Hurtmans, D., Turquety, S., George, M., Hadji-Lazaro, J., Keim, C., and Meyer-Arnek, J.: Measurements of total and tropospheric ozone from IASI: comparison with correlative satellite, ground-based and ozonesonde observations, *Atmos. Chem. Phys.*, 9, 6255–6271, doi:10.5194/acp-9-6255-2009, 2009.
- Capelle, V., Chédin, A., Péquignot, E., Schluessel, P., Newman, S. M., and Scott, N. A.: Infrared continental surface emissivity spectra and skin temperature retrieved from IASI observations over the tropics, *J. Appl. Meteorol. Clim.*, 51, 1164–1179, doi:10.1175/JAMC-D-11-0145.1, 2012.

Towards IASI-New Generation (IASI-NG): impact of improved spectral resolution

C. Crevoisier et al.

Title Page

Abstract

Introduction

Conclusions

References

Tables

Figures

⏪

⏩

◀

▶

Back

Close

Full Screen / Esc

Printer-friendly Version

Interactive Discussion



Towards IASI-New Generation (IASI-NG): impact of improved spectral resolution

C. Crevoisier et al.

Title Page

Abstract

Introduction

Conclusions

References

Tables

Figures

◀

▶

◀

▶

Back

Close

Full Screen / Esc

Printer-friendly Version

Interactive Discussion

- Collard, A. D. and McNally, A. P.: The assimilation of Infrared Atmospheric Sounding Interferometer radiances at ECMWF, *Q. J. Roy. Meteorol. Soc.*, 135, 1044–1058, 2009.
- Crevoisier, C., Chédin, A., and Scott, N. A.: AIRS channel selection for CO₂ and other trace-gas retrievals, *Q. J. Roy. Meteorol. Soc.*, 129, 2719–2740, 2003.
- 5 Crevoisier, C., Chédin, A., Matsueda, H., Machida, T., Armante, R., and Scott, N. A.: First year of upper tropospheric integrated content of CO₂ from IASI hyperspectral infrared observations, *Atmos. Chem. Phys.*, 9, 4797–4810, doi:10.5194/acp-9-4797-2009, 2009a.
- Crevoisier, C., Nobileau, D., Fiore, A. M., Armante, R., Chédin, A., and Scott, N. A.: Tropospheric methane in the tropics – first year from IASI hyperspectral infrared observations, *Atmos. Chem. Phys.*, 9, 6337–6350, doi:10.5194/acp-9-6337-2009, 2009b.
- 10 Crevoisier, C., Nobileau, D., Armante, R., Crépeau, L., Machida, T., Sawa, Y., Matsueda, H., Schuck, T., Thonat, T., Pernin, J., Scott, N. A., and Chédin, A.: The 2007–2011 evolution of tropical methane in the mid-troposphere as seen from space by MetOp-A/IASI, *Atmos. Chem. Phys.*, 13, 4279–4289, doi:10.5194/acp-13-4279-2013, 2013.
- 15 De Wachter, E., Barret, B., Le Flochmoën, E., Pavelin, E., Matricardi, M., Clerbaux, C., Hadji-Lazaro, J., George, M., Hurtmans, D., Coheur, P.-F., Nedelec, P., and Cammas, J. P.: Retrieval of MetOp-A/IASI CO profiles and validation with MOZAIC data, *Atmos. Meas. Tech.*, 5, 2843–2857, doi:10.5194/amt-5-2843-2012, 2012.
- Duflot, V., Hurtmans, D., Clarisse, L., R'honi, Y., Vigouroux, C., De Mazière, M., Mahieu, E., Servais, C., Clerbaux, C., and Coheur, P.-F.: Measurements of hydrogen cyanide (HCN) and acetylene (C₂H₂) from the Infrared Atmospheric Sounding Interferometer (IASI), *Atmos. Meas. Tech.*, 6, 917–925, doi:10.5194/amt-6-917-2013, 2013.
- 20 Dufour, G., Eremenko, M., Griesfeller, A., Barret, B., LeFlochmoën, E., Clerbaux, C., Hadji-Lazaro, J., Coheur, P.-F., and Hurtmans, D.: Validation of three different scientific ozone products retrieved from IASI spectra using ozonesondes, *Atmos. Meas. Tech.*, 5, 611–630, doi:10.5194/amt-5-611-2012, 2012.
- 25 Edwards, D. P., Arellano, A. F., and Deeter, M. N.: A satellite observation system simulation experiment for carbon monoxide in the lowermost troposphere, *J. Geophys. Res.*, 114, D14304, doi:10.1029/2008JD011375, 2009.
- 30 Eremenko, M., Dufour, G., Foret, G., Keim, C., Orphal, J., Beekmann, M., Bergametti, G., and Flaud, J.-M.: Tropospheric ozone distributions over Europe during the heat wave in July 2007 observed from infrared nadir spectra recorded by IASI, *Geophys. Res. Lett.*, 35, L18805, doi:10.1029/2008GL034803, 2008.

Towards IASI-New Generation (IASI-NG): impact of improved spectral resolution

C. Crevoisier et al.

Title Page

Abstract

Introduction

Conclusions

References

Tables

Figures

◀

▶

◀

▶

Back

Close

Full Screen / Esc

Printer-friendly Version

Interactive Discussion

EUMETSAT: Post-EPS Mission Requirements Document, EUM/PEPS/REQ/06/0043, v3A, <http://www.yumpu.com/en/document/view/10320570/post-eps-mission-requirements-document-pdf-3-mb-eumetsat> (last access: 9 December 2013), 22 January 2010.

GCOS-107: Systematic observation requirements for satellite-based products for climate, Supplemental details to the satellite-based component of the “Implementation Plan for the Global Observing System for Climate in Support of the UNFCCC”, September 2006, WMO/TD No. 1338, available at: <http://www.wmo.int/pages/prog/gcos/Publications/gcos-107.pdf>, last access: 9 December 2013, WMO – World Meteorological Organization, Intergovernmental Oceanographic Commission, United Nations Environment Programme, and International Council for Science, 2006.

GCOS-154: Systematic observation requirements for satellite-based products for climate – 2011 update, December 2011, available at: <http://www.wmo.int/pages/prog/gcos/Publications/gcos-154.pdf>, last access: 9 December 2013, WMO – World Meteorological Organization, Intergovernmental Oceanographic Commission, United Nations Environment Programme, and International Council for Science, 2011.

George, M., Clerbaux, C., Hurtmans, D., Turquety, S., Coheur, P.-F., Pommier, M., Hadji-Lazaro, J., Edwards, D. P., Worden, H., Luo, M., Rinsland, C., and McMillan, W.: Carbon monoxide distributions from the IASI/METOP mission: evaluation with other space-borne remote sensors, *Atmos. Chem. Phys.*, 9, 8317–8330, doi:10.5194/acp-9-8317-2009, 2009.

Guidard, V., Fourrié, N., Brousseau, P., and Rabier, F.: Impact of IASI assimilation at global and convective scales and challenges for the assimilation of cloudy scenes, *Q. J. Roy. Meteorol. Soc.*, 137, 1975–1987, doi:10.1002/qj.928, 2011.

Herbin, H., Hurtmans, D., Turquety, S., Wespes, C., Barret, B., Hadji-Lazaro, J., Clerbaux, C., and Coheur, P.-F.: Global distributions of water vapour isotopologues retrieved from IMG/ADEOS data, *Atmos. Chem. Phys.*, 7, 3957–3968, doi:10.5194/acp-7-3957-2007, 2007.

Herbin, H., Hurtmans, D., Clerbaux, C., Clarisse, L., and Coheur, P.-F.: H_2^{16}O and HDO measurements with IASI/MetOp, *Atmos. Chem. Phys.*, 9, 9433–9447, doi:10.5194/acp-9-9433-2009, 2009.

Hólm, E., Andersson, E., Beljaars, A., Lopez, P., Mahfouf, J.-F., Simmons, A. J., and Thépaut, J.-N.: Assimilation and modelling of the hydrological cycle: ECMWF’s Status and Plan, ECMWF Tech. Memo. 383, ECMWF, 2002.

Towards IASI-New Generation (IASI-NG): impact of improved spectral resolution

C. Crevoisier et al.

Title Page

Abstract

Introduction

Conclusions

References

Tables

Figures

◀

▶

◀

▶

Back

Close

Full Screen / Esc

Printer-friendly Version

Interactive Discussion

- Hilton, F., Armante, R., August, T., Barnet, C., Bouchard, A., Camy-Peyret, C., Capelle, V., Clarisse, L., Clerbaux, C., Coheur, P.-F., Collard, A., Crevoisier, C., Dufour, G., and Edwards, D. Fajjan, F., Fourrié, N., Gambacorta, A., Goldberg, M., Guidard, V., Hurtmans, D., Illingworth, S., Jacquinet-Husson, N., Kerzenmacher, T., Klaes, D., Lavanant, L., Masiello, G., Matricardi, M., McNally, A., Newman, S., Pavelin, E., Payan, S., Pequignot, E., Peyridieu, S., Phulpin, T., Remedios, J., Schlüssel, P., Serio, C., Strow, L., Stubenrauch, C., Taylor, J., Tobin, D., Wolf, W., and Zhou, D., Hyperspectral Earth Observation from IASI: Five Years of Accomplishments, *B. Am. Meteorol. Soc.*, 93, 347–370, doi:10.1175/BAMS-D-11-00027.1, 2012.
- Hurtmans, D., Coheur, P.-F., Wespes, C., Clarisse, L., Scharf, O., Clerbaux, C., Hadji-Lazaro, J., George, M., and Turquety, S.: FORLI radiative transfer and retrieval code for IASI, *J. Quant. Spectrosc. Ra.*, 113, 1391–1408, 2012.
- Jacquinet-Husson, N., Crepeau, L., Armante, R., Boutammine, C., Chédin, A., Scott, N. A., Crevoisier, C., Capelle, V., Boone, C., Poulet-Crovisier, N., Barbe, A., Campargue, A., Chris Benner, D., Benilan, Y., Bézard, B., Boudon, V., Brown, L. R., Coudert, L. H., Coustenis, A., Dana, V., Devi, V. M., Fally, S., Fayt, A., Flaud, J.-M., Goldman, A., Herman, M., Harrio, G. J., Jacquemart, D., Jolly, A., Kleiner, I., Kleinböhl, A., Kwabia-Tchana, F., Lavrentieva, N., Lacombe, N., Li-Hong, X., Lyulin, O. M., Mandin, J.-Y., Maki, A., Mikhailenko, S., Miller, C. E., Mishina, T., Moazzen-Ahmadi, N., Müller, H. S. P., Nikitin, A., Orphal, J., Perevalov, V., Perrin, A., Petkie, D. T., Predoi-Cross, A., Rinsland, C. P., Remedios, J. J., Rotger, M., Smith, M. A. H., Sung, K., Tashkun, S., Tennyson, J., Toth, R. A., Vandaele, A.-C., and Vander Auwera, J.: The 2009 edition of the GEISA spectroscopic database, *J. Quant. Spectrosc. Ra.*, 112, 2395–2445, doi:10.1016/j.jqsrt.2011.06.004, 2011.
- Kerzenmacher, T., Dils, B., Kumps, N., Blumenstock, T., Clerbaux, C., Coheur, P.-F., Demoulin, P., García, O., George, M., Griffith, D. W. T., Hase, F., Hadji-Lazaro, J., Hurtmans, D., Jones, N., Mahieu, E., Notholt, J., Paton-Walsh, C., Raffalski, U., Ridder, T., Schneider, M., Servais, C., and De Mazière, M.: Validation of IASI FORLI carbon monoxide retrievals using FTIR data from NDACC, *Atmos. Meas. Tech.*, 5, 2751–2761, doi:10.5194/amt-5-2751-2012, 2012.
- Klüser, L., Kleiber, P., Holzer-Popp, T., and Grassia, V. H.: Desert dust observation from space – Application of measured mineral component infrared extinction spectra, *Atmos. Environ.*, 54, 419–427, doi:10.1016/j.atmosenv.2012.02.011, 2012.

Towards IASI-New Generation (IASI-NG): impact of improved spectral resolution

C. Crevoisier et al.

Title Page

Abstract

Introduction

Conclusions

References

Tables

Figures

⏪

⏩

◀

▶

Back

Close

Full Screen / Esc

Printer-friendly Version

Interactive Discussion

- Kulawik, S. S., Osterman, G., Jones, D. B. A., and Bowman, K. W.: Calculation of altitude-dependent Tikhonov constraints for TES nadir retrievals, *IEEE T. Geosci. Remote* 44, 1334–1342, 2006.
- 5 Kwon, E.-H., Sohn, B. J., Smith, W. L., and Li, J.: Validating IASI Temperature and Moisture Sounding Retrievals over East Asia Using Radiosonde Observations, *J. Atmos. Ocean. Tech.*, 29, 1250–1262, doi:10.1175/JTECH-D-11-00078.1, 2012.
- Lacour, J.-L., Risi, C., Clarisse, L., Bony, S., Hurtmans, D., Clerbaux, C., and Coheur, P.-F.: Mid-tropospheric δD observations from IASI/MetOp at high spatial and temporal resolution, *Atmos. Chem. Phys.*, 12, 10817–10832, doi:10.5194/acp-12-10817-2012, 2012.
- 10 Lamquin, N., Stubenrauch, C. J., Gierens, K., Burkhardt, U., and Smit, H.: A global climatology of upper-tropospheric ice supersaturation occurrence inferred from the Atmospheric Infrared Sounder calibrated by MOZAIC, *Atmos. Chem. Phys.*, 12, 381–405, doi:10.5194/acp-12-381-2012, 2012.
- Lezeaux, O., Pierangelo, C., Scott, N. A., Camy-Peyret, C., Cassé, V., Klonecki, A., Prunet, P., Payan, S., Armante, R., Capelle, V., and Phulpin, T.: Temperature sounding from IASI using N_2O channels: Theoretical study and validation with JAIVEx observations, 2nd IASI International Conference, Annecy, 25–29 January 2010, France, 2010.
- 15 Niro, F., Boulet, C., and Hartmann, J.-M.: Spectra calculations in central and wing regions of CO_2 IR bands between 10 and 20 μm , I: model and laboratory measurements, *J. Quant. Spectrosc. Ra.*, 88, 483–498, doi:10.1016/j.jqsrt.2004.04.003, 2004a.
- 20 Niro, F., von Clarmann, T., Jucks, K., and Hartmann, J.-M.: Spectra calculations in central and wing regions of CO_2 IR bands between 10 and 20 μm , III: atmospheric emission spectra, *J. Quant. Spectrosc. Ra.*, 90, 61–76, doi:10.1016/j.jqsrt.2004.04.005, 2004b.
- Péquignot, E., Chédin, A., and Scott, N. A.: Infrared continental surface emissivity spectra retrieved from AIRS hyperspectral sensor, *J. Appl. Meteorol. Clim.*, 47, 1619–1633, 2008.
- 25 Peyridieu, S., Chédin, A., Capelle, V., Tsamalis, C., Pierangelo, C., Armante, R., Crevoisier, C., Crépeau, L., Siméon, M., Ducos, F., and Scott, N. A.: Characterisation of dust aerosols in the infrared from IASI and comparison with PARASOL, MODIS, MISR, CALIOP, and AERONET observations, *Atmos. Chem. Phys.*, 13, 6065–6082, doi:10.5194/acp-13-6065-2013, 2013.
- 30 Pougatchev, N., August, T., Calbet, X., Hultberg, T., Oduleye, O., Schlüssel, P., Stiller, B., Germain, K. St., and Bingham, G.: IASI temperature and water vapor retrievals – error assessment and validation, *Atmos. Chem. Phys.*, 9, 6453–6458, doi:10.5194/acp-9-6453-2009, 2009.

Towards IASI-New Generation (IASI-NG): impact of improved spectral resolution

C. Crevoisier et al.

Title Page

Abstract

Introduction

Conclusions

References

Tables

Figures

⏪

⏩

◀

▶

Back

Close

Full Screen / Esc

Printer-friendly Version

Interactive Discussion

- Razavi, A., Karagulian, F., Clarisse, L., Hurtmans, D., Coheur, P. F., Clerbaux, C., Müller, J. F., and Stavrou, T.: Global distributions of methanol and formic acid retrieved for the first time from the IASI/MetOp thermal infrared sounder, *Atmos. Chem. Phys.*, 11, 857–872, doi:10.5194/acp-11-857-2011, 2011.
- 5 R'Honi, Y., Clarisse, L., Clerbaux, C., Hurtmans, D., Duflot, V., Turquety, S., Ngadi, Y., and Coheur, P.-F.: Exceptional emissions of NH_3 and HCOOH in the 2010 Russian wildfires, *Atmos. Chem. Phys.*, 13, 4171–4181, doi:10.5194/acp-13-4171-2013, 2013.
- Rodgers, C. D.: *Inverse Methods for Atmospheric Sounding: Theory and Practice*, World Sci., Hackensack, N. J., 2000.
- 10 Rumelhart, D. E., Hinton, G. E., and Williams, R. J.: Learning internal representations by error propagation, in: *Parallel Distributed Processing: Explorations in the Macrostructure of Cognition*, vol. 1, edited by: Rumelhart, D. E. and McClelland, J. L., MIT Press, Cambridge, Mass., 318–362, 1986.
- Scott, N. A. and Chédin, A.: A fast line-by-line method for atmospheric absorption computations: The Automatized Atmospheric Absorption Atlas, *J. Appl. Meteorol.*, 20, 802–812, 1981.
- 15 Sellitto, P., Dufour, G., Eremenko, M., Cuesta, J., Dauphin, P., Forêt, G., Gaubert, B., Beekmann, M., Peuch, V.-H., and Flaud, J.-M.: Analysis of the potential of one possible instrumental configuration of the next generation of IASI instruments to monitor lower tropospheric ozone, *Atmos. Meas. Tech.*, 6, 621–635, doi:10.5194/amt-6-621-2013, 2013.
- 20 Stubenrauch, C., Feofilov, A., Armante, R., and Guignard, A.: Cloud properties & bulk microphysical properties of semi-transparent cirrus from AIRS & IASI, Third IASI International Conference, 4–8 February, Hyères, 2013.
- Thonat, T., Crevoisier, C., Scott, N. A., Chédin, A., Schuck, T., Armante, R., and Crépeau, L.: Retrieval of tropospheric CO column from hyperspectral infrared sounders – application to four years of Aqua/AIRS and MetOp-A/IASI, *Atmos. Meas. Tech.*, 5, 2413–2429, doi:10.5194/amt-5-2413-2012, 2012.
- 25 Worden, J., Bowman, K., Noone, D., Beer, R., Clough, S., Eldering, A., Fisher, B., Goldman, A., Gunson, M., Herman, R., Kulawik, S., Lampel, M., Luo, M., Osterman, G., Rinsland, C., Rodgers, C., Sander, S., Shephard, M., and Worden, H.: Tropospheric Emission Spectrometer observations of the tropospheric $\text{HDO}/\text{H}_2\text{O}$ ratio: Estimation approach and characterization, 25 August, *J. Geophys. Res.*, 111, D16309, doi:10.1029/2005JD006606, 2006.
- 30

Towards IASI-New Generation (IASI-NG): impact of improved spectral resolution

C. Crevoisier et al.

Title Page

Abstract

Introduction

Conclusions

References

Tables

Figures

◀

▶

◀

▶

Back

Close

Full Screen / Esc

Printer-friendly Version

Interactive Discussion



Worden, H. M., Logan, J. A., Worden, J. R., Beer, R., Bowman, K., Clough, S. A., Eldering, A., Fisher, B. M., Gunson, M. R., Herman, R. L., Kulawik, S. S., Lampel, M. C., Luo, M., Megret-skaia, I. A., Osterman, G. B., and Shephard, M. W.: Comparisons of Tropospheric Emission Spectrometer (TES) ozone profiles to ozonesondes: Methods and initial results, *J. Geophys. Res.*, 112, D03309, doi:10.1029/2006JD007258, 2007.

Zakharov, V. I., Imasu, R., Gribanov, K. G., Hoffmann, G., and Jouzel, J.: Latitudinal distribution of the deuterium to hydrogen ratio in the atmospheric water vapour retrieved from IMG/ADEOS data, *Geophys. Res. Lett.*, 31, L12104, doi:10.1029/2004GL019433, 2004.

Zhou, D. K., Larar, A. M., Liu, X., Smith, W. L., Strow, L. L., Yang, P., Schlüssel, P., and Calbet, X.: Global land surface emissivity retrieved from satellite ultraspectral IR measurements, *IEEE T. Geosci. Remote*, 49, 1277–1290, doi:10.1109/TGRS.2010.2051036, 2011.

Towards IASI-New Generation (IASI-NG): impact of improved spectral resolution

C. Crevoisier et al.

Table 1. The 6 Infrared Sounder (IRS) scenarios.

Spectral resolution	IASI noise	IASI noise/2	IASI noise/4
IASI (0.5 cm^{-1})	IRS1a (IASI)	IRS1b	IRS1c
IASI-NG (0.25 cm^{-1})	IRS2a	IRS2b	IRS2c

Title Page

Abstract

Introduction

Conclusions

References

Tables

Figures

◀

▶

◀

▶

Back

Close

Full Screen / Esc

Printer-friendly Version

Interactive Discussion

Towards IASI-New Generation (IASI-NG): impact of improved spectral resolution

C. Crevoisier et al.

Table 2. Number of degrees of freedom for the retrieval of temperature profile for the 8 scenarios, using all the channels located in the 645–770 cm^{-1} range, or a combination of both the 645–770 cm^{-1} and the 2250–2420 cm^{-1} ranges.

	IRS1a	IRS1b	IRS1c	IRS2a	IRS2b	IRS2c
645–770 cm^{-1}	3.2	5.6	7.1	4.4	7.7	9.8
645–770 cm^{-1} and 2250–2420 cm^{-1}	3.3	5.8	7.3	4.6	8.0	10.0

[Title Page](#)
[Abstract](#)
[Introduction](#)
[Conclusions](#)
[References](#)
[Tables](#)
[Figures](#)




[Back](#)
[Close](#)
[Full Screen / Esc](#)
[Printer-friendly Version](#)
[Interactive Discussion](#)


Towards IASI-New Generation (IASI-NG): impact of improved spectral resolution

C. Crevoisier et al.

Table 4. Impact of spectral resolution, radiometric noise on the accuracy of the retrieval of CO₂ tropospheric columns, expressed relative to the IRS1a/IASI accuracy (%). Three spectral ranges are used: either the 15 μm band, or the 4.3 μm band or both bands. Note that IRS1a/IASI and IRS2a CO₂ retrievals are only performed with the 15 μm band.

	IRS1b	IRS1c	IRS2a	IRS2b	IRS2c
15 μm	10	24	9	30	40
4.3 μm	–	5	–	–7	14
15 and 4.3 μm	–	41	–	45	54

Title Page

Abstract

Introduction

Conclusions

References

Tables

Figures

◀

▶

◀

▶

Back

Close

Full Screen / Esc

Printer-friendly Version

Interactive Discussion



Towards IASI-New Generation (IASI-NG): impact of improved spectral resolution

C. Crevoisier et al.

Title Page

Abstract

Introduction

Conclusions

References

Tables

Figures

◀

▶

◀

▶

Back

Close

Full Screen / Esc

Printer-friendly Version

Interactive Discussion

Table 5. Impact of spectral resolution and radiometric noise on the accuracy of the retrieval of CH₄ tropospheric columns, expressed relative to the IRS1a-IASI accuracy (%).

	IRS1b	IRS1c	IRS2a	IRS2b	IRS2c
Gain (%)	5	9	39	44	47

Towards IASI-New Generation (IASI-NG): impact of improved spectral resolution

C. Crevoisier et al.

Title Page

Abstract

Introduction

Conclusions

References

Tables

Figures

◀

▶

◀

▶

Back

Close

Full Screen / Esc

Printer-friendly Version

Interactive Discussion



Table 7. Vertical information expressed in DOFs of the CO retrievals for each scenario.

	IRS1a	IRS1b	IRS1c	IRS2a	IRS2b	IRS2c
DOFs	1.84	2.20	2.6	2.28	2.65	2.98

AMTD

6, 11215–11277, 2013

Towards IASI-New Generation (IASI-NG): impact of improved spectral resolution

C. Crevoisier et al.

Title Page

Abstract

Introduction

Conclusions

References

Tables

Figures

◀

▶

◀

▶

Back

Close

Full Screen / Esc

Printer-friendly Version

Interactive Discussion

Table 9. Vertical information expressed in DOFs of the ozone retrievals for each scenario.

	IRS1a	IRS1b	IRS1c	IRS2a	IRS2b	IRS2c
DOFs	3.59	4.10	4.65	3.97	4.70	5.45

Towards IASI-New Generation (IASI-NG): impact of improved spectral resolution

C. Crevoisier et al.

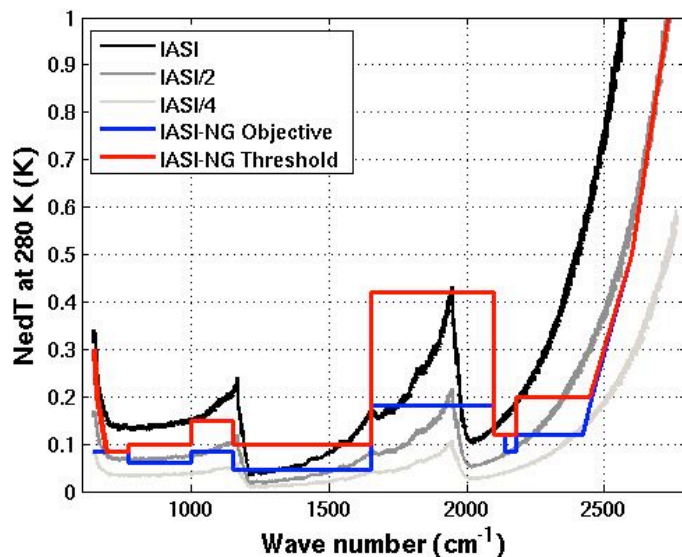


Fig. 1. Radiometric noise expressed as level 1c equivalent noise temperature $NE\Delta T$ for a reference temperature of 280 K. The black line gives the in-flight measured IASI noise. Grey lines give the IASI noise when divided by a factor of 2 and 4. The current noise specifications for IASI-NG are plotted in red (threshold specification) and in blue (objective specification).

Title Page

Abstract

Introduction

Conclusions

References

Tables

Figures

⏪

⏩

◀

▶

Back

Close

Full Screen / Esc

Printer-friendly Version

Interactive Discussion

Towards IASI-New Generation (IASI-NG): impact of improved spectral resolution

C. Crevoisier et al.

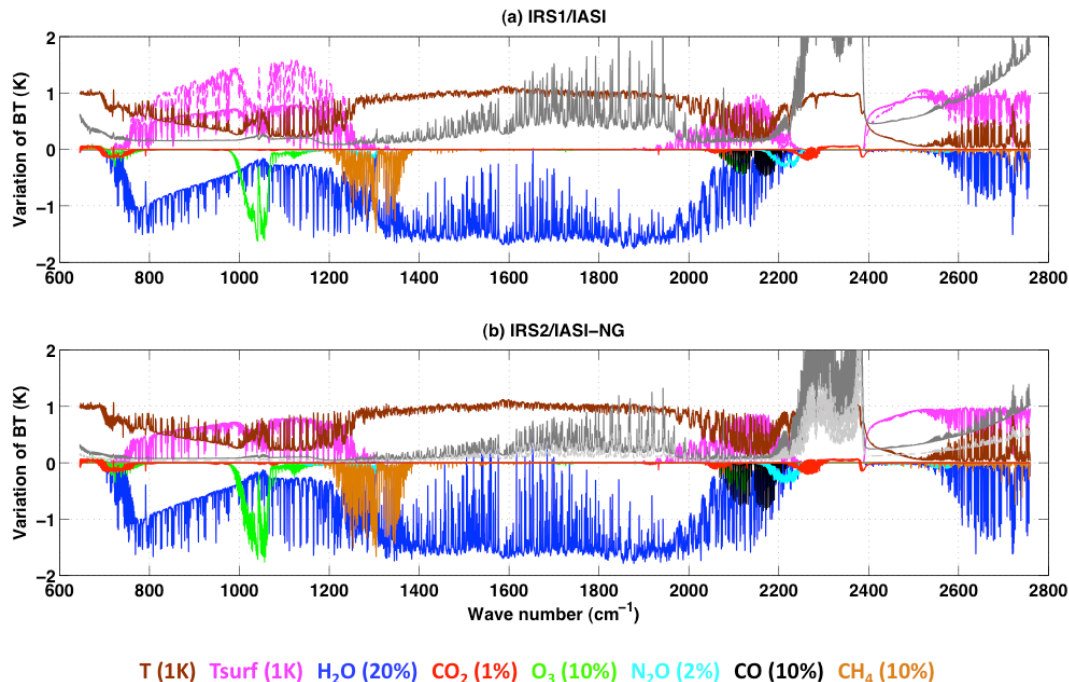


Fig. 2. Sensitivities of infrared channels at the spectral resolution of IRS1/IASI **(a)** and IRS2/IASI-NG **(b)** to various atmospheric and surface variables and averaged over the whole tropical TIGR atmospheric situations. Variations of 1 K of temperature (brown), 20 % of water vapour (blue), 1 % of CO₂ (red), 10 % of O₃ (green), 2 % of N₂O (cyan), 10 % of CO (black), 10 % of CH₄ (orange) and 1 K of surface temperature (pink). Also shown is the radiometric noise of each scenario computed at the BT of the channels (grey): IASI noise in **(a)** and IASI noise divided by 2 (dark grey in **(b)**) and by 4 (light grey in **(b)**). The computation of channels sensitivities is based on simulations performed using the forward radiative transfer model 4A/OP (Scott and Chédin, 1981; <http://4aop.noveltis.com/>) based on the GEISA09 spectroscopic database (Jacquinet-Husson et al., 2011).

Towards IASI-New Generation (IASI-NG): impact of improved spectral resolution

C. Crevoisier et al.

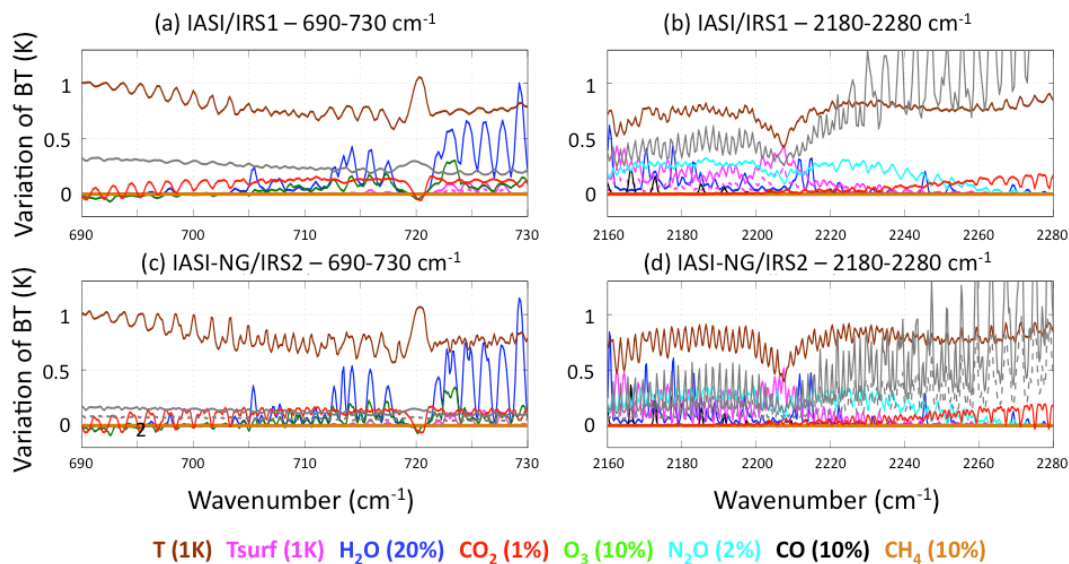


Fig. 3. Same as Fig. 2 for the two spectral bands 690–730 and 2180–2280 cm^{-1} . To ease the comparison between the various signals, a factor of -1 has been applied to variations of BT for all the gases.

[Title Page](#)
[Abstract](#)
[Introduction](#)
[Conclusions](#)
[References](#)
[Tables](#)
[Figures](#)
[◀](#)
[▶](#)
[◀](#)
[▶](#)
[Back](#)
[Close](#)
[Full Screen / Esc](#)
[Printer-friendly Version](#)
[Interactive Discussion](#)

Towards IASI-New Generation (IASI-NG): impact of improved spectral resolution

C. Crevoisier et al.

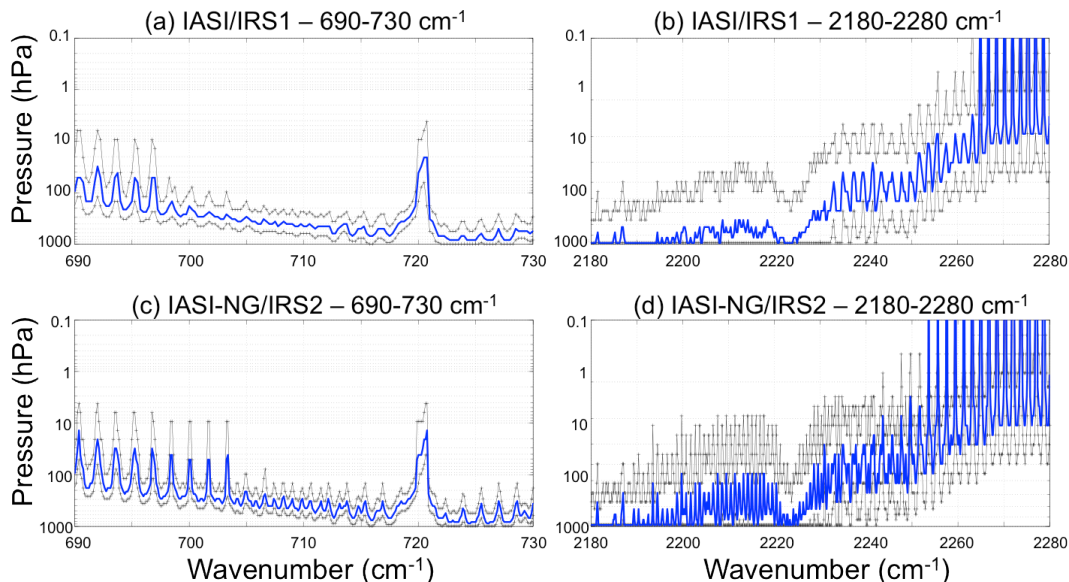


Fig. 4. Pressure of the maximum (blue line) and of the half-height width (black) of the temperature Jacobians at the IASI spectral resolution in the $15\ \mu\text{m}$ (a) and $4.3\ \mu\text{m}$ (b) bands and at the IASI-NG spectral resolution in the $15\ \mu\text{m}$ (c) and $4.3\ \mu\text{m}$ (d) bands. The Jacobians have been computed by 4A and averaged over the whole tropical atmospheric situations of the TIGR database.

Towards IASI-New Generation (IASI-NG): impact of improved spectral resolution

C. Crevoisier et al.

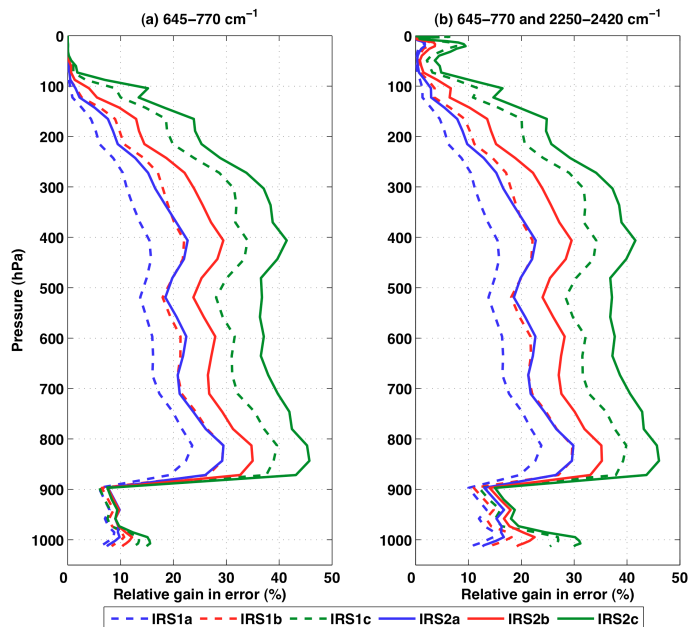


Fig. 5. Impact of spectral resolution and radiometric noise on the retrieval of temperature profile based on the use of the $645\text{--}770\text{ cm}^{-1}$ spectral band **(a)** or of the $645\text{--}770$ and $2250\text{--}2420\text{ cm}^{-1}$ spectral bands combined **(b)**. The relative gain in error is defined as the difference between the a priori and a posteriori error, divided by the a priori error, averaged over the whole tropical TIGR situations.

**Towards IASI-New Generation (IASI-NG):
impact of improved
spectral resolution**

C. Crevoisier et al.

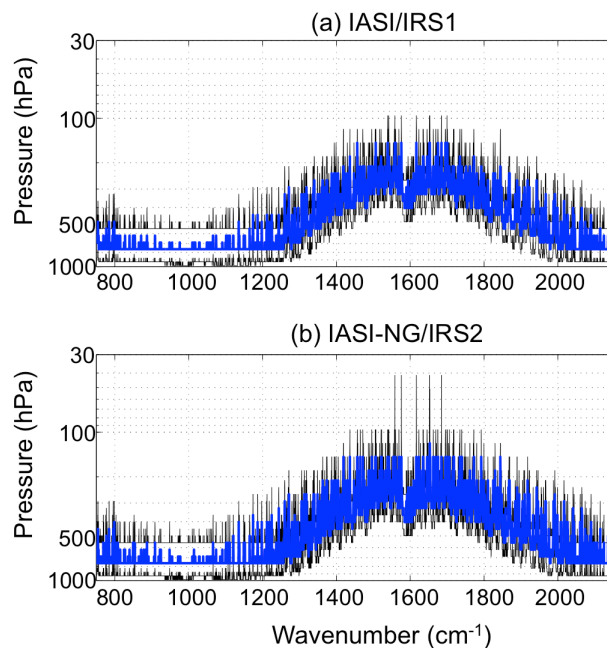


Fig. 6. Pressure of the maximum (blue line) and of the half-height width (black) of the H_2O Jacobians at the IASI spectral resolution (upper panel) and at the IASI-NG spectral resolution (bottom panel). Average over the TIGR tropical atmospheric situations.

Towards IASI-New Generation (IASI-NG): impact of improved spectral resolution

C. Crevoisier et al.

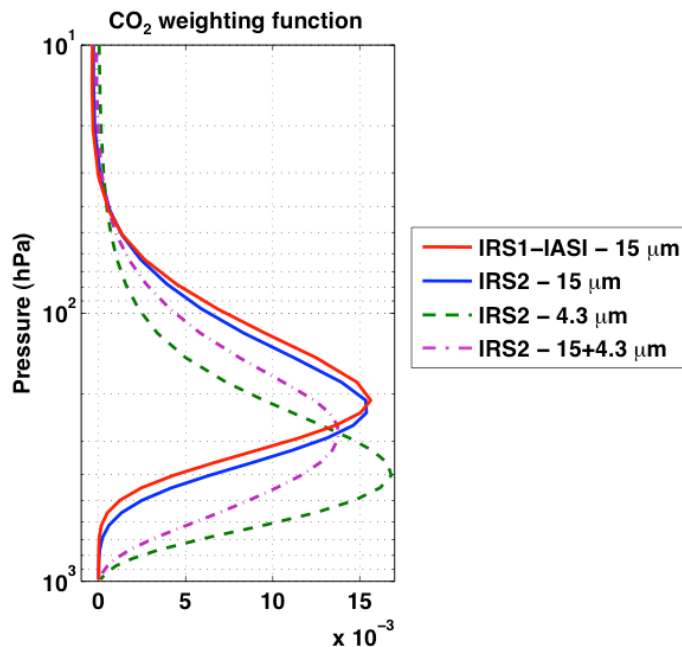


Fig. 8. CO₂ weighting function associated with the retrieval for IRS1 scenarios using the channels located in the 15 μm CO₂ absorption band only (red) and for the IRS2 scenarios using the channels located either in the 15 μm CO₂ absorption band (blue), in the 4.3 μm CO₂ absorption band (dashed green), or in both bands (dot-dashed purple).

Towards IASI-New Generation (IASI-NG): impact of improved spectral resolution

C. Crevoisier et al.

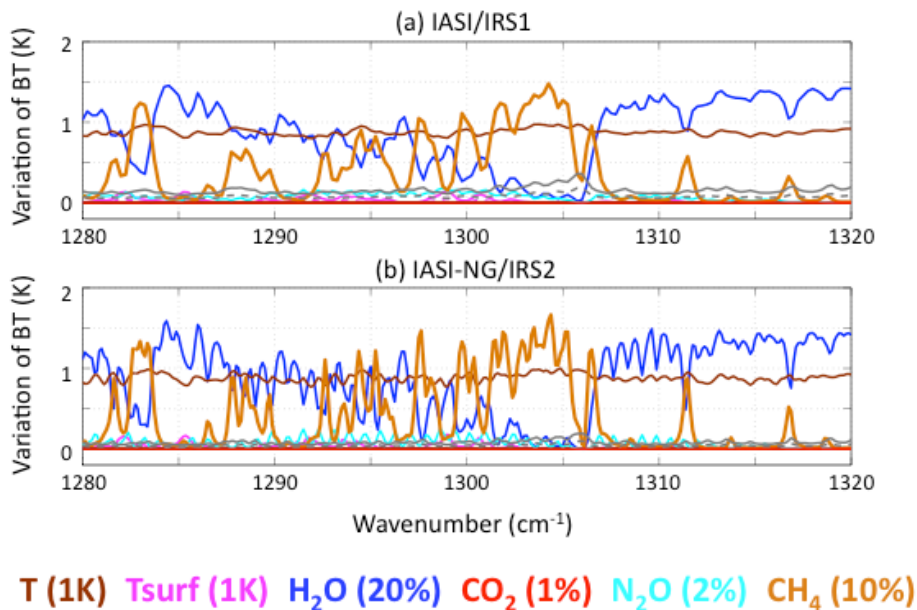


Fig. 9. Same as Fig. 2 for the CH₄ ν₄ absorption band.

Towards IASI-New Generation (IASI-NG): impact of improved spectral resolution

C. Crevoisier et al.

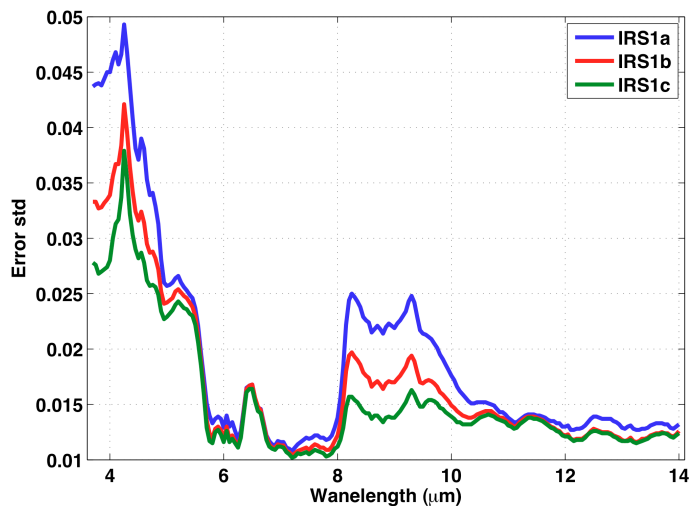


Fig. 10. Impact of radiometric noise on the retrieval of surface spectral emissivity: standard deviation of retrieved emissivity for IRS1a-IASI (blue), IRS1b (red), IRS1c (green).

[Title Page](#)[Abstract](#)[Introduction](#)[Conclusions](#)[References](#)[Tables](#)[Figures](#)[⏪](#)[⏩](#)[◀](#)[▶](#)[Back](#)[Close](#)[Full Screen / Esc](#)[Printer-friendly Version](#)[Interactive Discussion](#)

**Towards IASI-New Generation (IASI-NG):
impact of improved
spectral resolution**

C. Crevoisier et al.

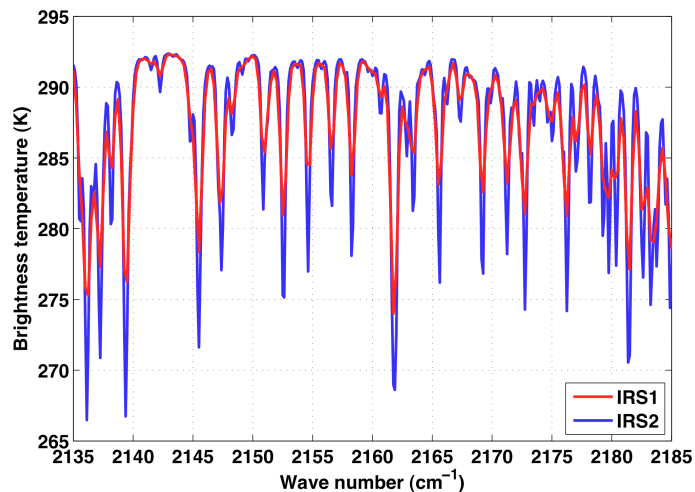


Fig. 11. Impact of spectral resolution on the CO lines in the 2135–2185 cm^{-1} spectral range used for the CO retrieval. Average over the whole tropical TIGR situations.

[Title Page](#)[Abstract](#)[Introduction](#)[Conclusions](#)[References](#)[Tables](#)[Figures](#)[⏪](#)[⏩](#)[◀](#)[▶](#)[Back](#)[Close](#)[Full Screen / Esc](#)[Printer-friendly Version](#)[Interactive Discussion](#)

**Towards IASI-New Generation (IASI-NG):
impact of improved
spectral resolution**

C. Crevoisier et al.

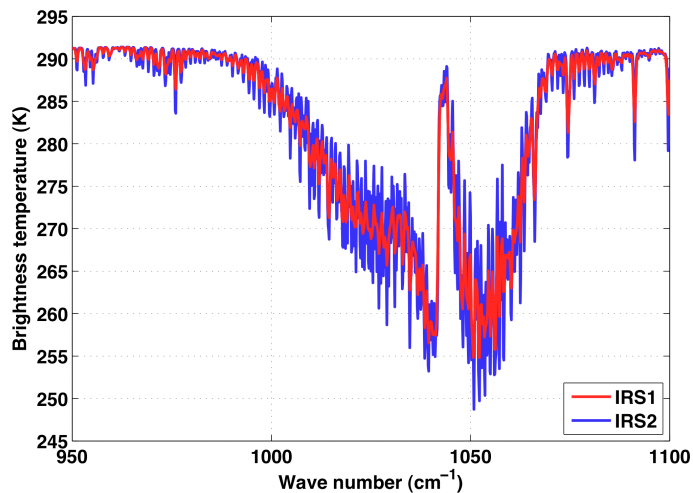


Fig. 13. Impact of spectral resolution on the ozone lines in the $950\text{--}1100\text{ cm}^{-1}$ spectral range used for the ozone retrieval. Average over the whole tropical TIGR situations.

[Title Page](#)[Abstract](#)[Introduction](#)[Conclusions](#)[References](#)[Tables](#)[Figures](#)[⏪](#)[⏩](#)[◀](#)[▶](#)[Back](#)[Close](#)[Full Screen / Esc](#)[Printer-friendly Version](#)[Interactive Discussion](#)

**Towards IASI-New Generation (IASI-NG):
impact of improved
spectral resolution**

C. Crevoisier et al.

Title Page

Abstract

Introduction

Conclusions

References

Tables

Figures

◀

▶

◀

▶

Back

Close

Full Screen / Esc

Printer-friendly Version

Interactive Discussion

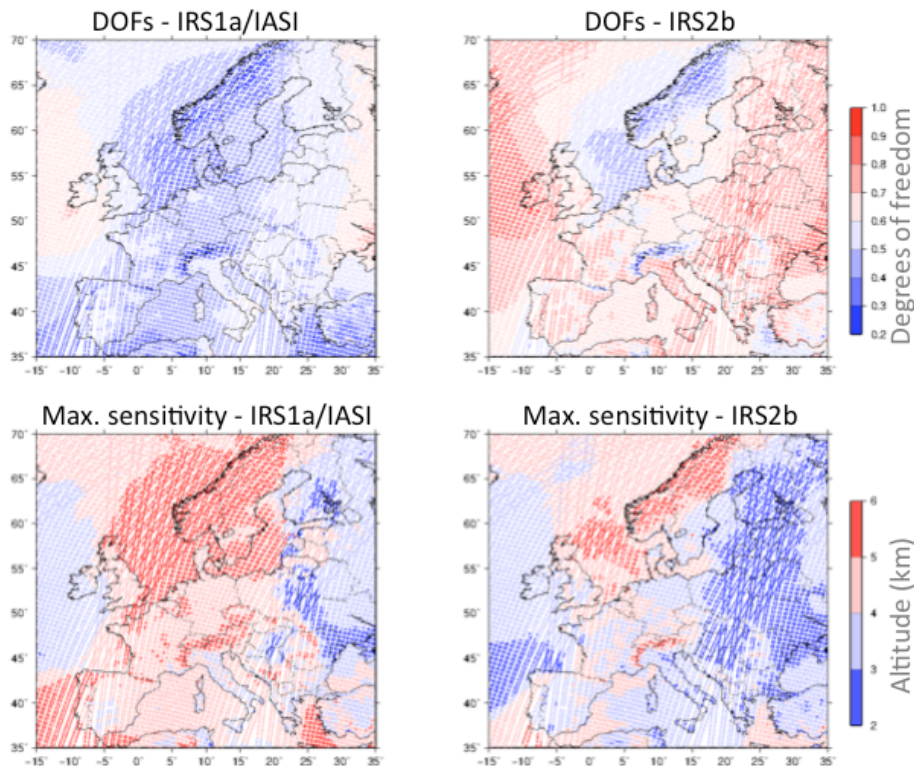


Fig. 14. DOFs (top panels) and altitude of the maximum sensitivity (bottom panels, in km) associated with the 0–6 km ozone retrieved on 20 August 2009, for IRS1a/IASI (left panels) and for the IRS2b scenario (right panels). This simulation was performed using a regional model that described an increase of ozone observed in Europe at that time. See Sellitto et al. (2013) for a full description of this case.

Towards IASI-New Generation (IASI-NG): impact of improved spectral resolution

C. Crevoisier et al.

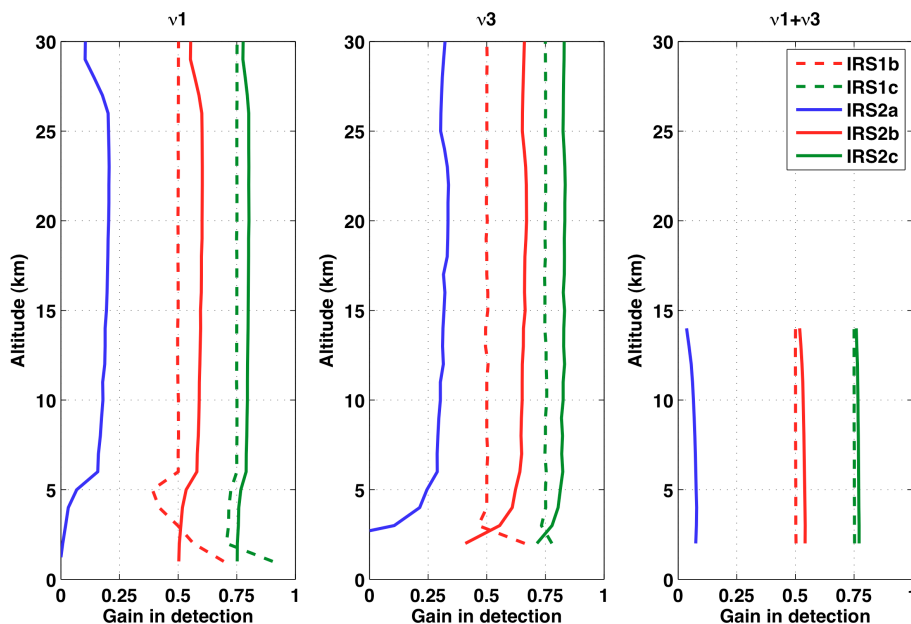


Fig. 15. Impact study on the detection limit for SO_2 . The plot represents the relative difference ratio between the detection limit of each scenario and the IRS1a-IASI scenario, as a function of altitude, for a case representative of a tropical atmospheric situation, when using the ν_1 band (left panel), ν_3 band (middle panel) and the $\nu_1 + \nu_3$ band (right panel). Note that the sensitivity of the latter band is limited to under 15 km.

**Towards IASI-New Generation (IASI-NG):
impact of improved
spectral resolution**

C. Crevoisier et al.

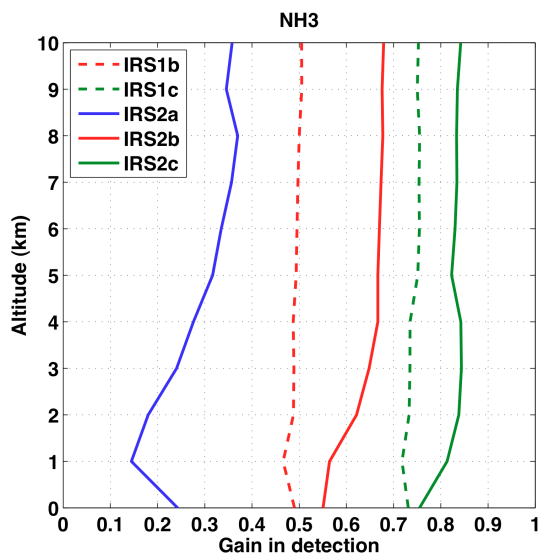


Fig. 16. Impact study on the detection limit for NH_3 . The plot represents the relative difference ratio between the detection limit of each scenario and the IRS1a-IASI scenario, as a function of altitude, for a case representative of a tropical atmospheric situation.